Superposition Model Analysis of Cr^{3+} ions Doped Cs$_2$CdCl$_4$ Single Crystal

Ram Kripal

EPR Laboratory, Department of Physics, University of Allahabad, Allahabad-211002, India

Abstract
Superposition model is applied to find zero field splitting parameters and crystal field parameters of Cr^{3+} doped Cs$_2$CdCl$_4$ single crystal. The zero field splitting parameters determined give good agreement with the experimental values when distortion is taken into account. The optical energy band positions for Cr^{3+} in Cs$_2$CdCl$_4$ are computed using crystal field parameters obtained from superposition model and Crystal Field Analysis package. The results suggest that Cr^{3+} ions substitute Cs$_2$CdCl$_4$ crystal at Cd^{2+} sites with charge compensation.
Keywords: *Superposition model; Crystal field: zero-field splitting; Optical spectroscopy; Cr^{3+} ions in Cs$_2$CdCl$_4$.*

I. Introduction

Electron paramagnetic resonance (EPR) provides information about the local site symmetry, zero field splitting (ZFS) parameters of transition ions and the defects responsible for the charge compensation in the doped crystals. In superposition model (SPM), the spin Hamiltonian parameters are found to result from contributions of nearest neighbours of the paramagnetic ion in the crystal. This model has been largely applied to find spin Hamiltonian parameters of various metal ions incorporated in crystals [1-6]

The EPR study of Cr^{3+} ion doped Cs$_2$CdCl$_4$ crystals [7, 8] at room temperature has been done earlier and the spin-Hamiltonian parameters determined [9]. The present study reports the SPM analysis of the zero field splitting parameters (ZFSPs) and the crystal field parameters (CFPs) for Cr^{3+} ions in Cs$_2$CdCl$_4$ single crystal. The objective is to obtain the ZFSPs, the CFPs and the structural distortion in the crystal for Cr^{3+} ions at different sites. The optical absorption energy band positions for Cr^{3+} ion in Cs$_2$CdCl$_4$ single crystal are computed using CFPs from SPM and crystal field analysis (CFA) package. The evaluated parameters may be applicable in various future studies for technological and industrial uses of different crystals.

This section provided the introduction of the subject and objective of the study performed. The remaining paper is organized as discussed below. Section II gives the related work associated with the SPM/ZFS and SPM/CF analysis. Section III describes the methods used for calculation of ZFSPs and CFPs. Section IV presents the results and its discussion. Section V provides conclusion and future scope of the study.

II. Crystal structure

The SPM/ZFS and SPM/CF analysis have been done for several ion-host systems [10-20]. The structure of Cs$_2$CdCl$_4$ crystal is tetragonal with a = 5.26 and c = 16.88 Å, Z = 2 [7]. The space group is *I4/mmm* and the crystal is isostructural with K$_2$NiF$_4$ [8]. Atoms are in the following positions: 4Cs in (e), z = 0.357, 2Cd in (a), 4Cl I in (c) and 4Cl II in (e), with z = 0.149. The site symmetry at Cr^{3+} ion is taken to be approximately orthorhombic. The orientations of the *(x, y, z)* axes (SAAS-symmetry adopted axis system) relative to the *(a, b, c)* crystallographic axes are *(x → a, y → b, z → c)* as shown in Fig. 1.

The structural data in spherical polar coordinates for the Cr^{3+} ions in Cs$_2$CdCl$_4$ single crystal on the basis of fractional coordinates of ligands [7] are given in Table 1. These data are used for SPM/ZFS and SPM/CF calculations in this study.

III. SPM calculations of ZFSPs

The spin Hamiltonian of transition ions in crystals is given by [10, 11, 12]:

$$\mathcal{H} = \mathcal{H}_{Ze} + \mathcal{H}_{ZFS} = \mu_B B.g.S + \sum B_k^q O_k^q = \mu_B B.g.S + \sum f_k b_k^q O_k^q , \qquad (1)$$

where g is the spectroscopic splitting factor, μ_B is the Bohr magneton, ***B*** is the applied magnetic field , S is the effective spin operator and $O_k^q (S_x, S_y, S_z)$ are the extended Stevens operators (ESO) [13, 14]. B_k^q and b_k^q

represent the ZFSPs, f_k = 1/3 and 1/60 are the scaling factors for k = 2 and 4, respectively. The ZFS terms in Eq. (1) for Cr³⁺ ion (S = 3/2) at orthorhombic symmetry sites are written as [15, 16, 17]:

$$\mathcal{H}_{ZFS} = B_2^0 O_2^0 + B_2^2 O_2^2 = \frac{1}{3} b_2^0 O_2^0 + \frac{1}{3} b_2^2 O_2^2 = D(S_z^2 - \frac{1}{3} S(S+1)) + E(S_x^2 - S_y^2),\qquad(2)$$

The conventional orthorhombic ZFSPs (D and E) and (B_k^q and b_k^q) have the relation:

$$b_2^0 = D = 3 B_2^0, \; b_2^2 = 3E = 3 B_2^2.\qquad(3)$$

From SPM [15-17], the ZFSPs for an ML$_n$ complex are obtained (in ESO notation) as:

$$b_k^q = \sum_i \bar{b}_k (R_0) \left(\frac{R_0}{R_i}\right)^{t_k} K_k^q (\theta_i, \varphi_i),\qquad(4)$$

where (R_i, θ_i, φ_i) are the spherical polar coordinates of the i-th ligand. The intrinsic parameters $\bar{b}_k$ (R_0) provide the strength of the k-th rank ZFS contribution from a ligand situated at the distance R_i, and the coordination factors K_k^q give the geometrical information [18]. K_k^q with k = 1 to 6 are given in Appendix A1 of [19]. t_k gives the power law exponent and R$_0$ is reference distance between metal and ligand.

Eq. (4) yields conventional ZFSPs, D and E as [19, 20-23]:

$$b_2^0 = D = \frac{\bar{b}_2(R_0)}{2}\left[\left(\frac{R_0}{R_i}\right)^{t_2} \sum_i (3\cos^2\theta_i - 1)\right]$$

$$\qquad(5)$$

$$b_2^2 = 3E = \frac{b_2^2}{3} = \frac{\bar{b}_2(R_0)}{2}\left[\left(\frac{R_0}{R_i}\right)^{t_2} \sum_i \sin^2\theta_i \cos 2\varphi_i\right]$$

Cr³⁺ ion in Cs₂CdCl₄ may be assumed to substitute at the Cd²⁺ ion site, and the interstitial site with similar ligand arrangement. The local symmetry at Cr³⁺ ion site is taken to be approximately orthorhombic. In octahedral coordination of Cr³⁺ ion for LiNbO₃ having Cr³⁺-O²⁻ bond, $\bar{b}_2(R_0)$ = 2.34 cm⁻¹ and t$_2$ = -0.12 have been used to find b_2^0 and b_2^2 [24]. Since Cr³⁺ ion in Cs₂CdCl₄ has distorted octahedral coordination (Fig.1) with chlorine as ligands, the b_K^q in the present analysis are found using the parameters $\bar{b}_2(R_0)$ = 2.34 cm⁻¹ and t$_2$ = -0.24.

The position of metal ion and spherical coordinates of ligands shown in Table 1 are used for calculation. The ZFSPs, D and E of Cr³⁺ ion in Cs₂CdCl₄ crystal are determined using Eq. (5). The reference distance of 0.200 nm was taken for the calculation [25], and the obtained values of ZFSPs are |D| = 0.0542 cm⁻¹ and |E| = 6.38E-07 cm⁻¹. The ratio b_2^2 / b_2^0 should be within the range (0, 1) for orthorhombic symmetry [26]. In the present study, the ratio $| b_2^2 | / | b_2^0 |$ = 3.53E-09 and |E| / |D| = 1.18E-09, which agrees with above. However, the values of |D| and |E| do not match with the experimental values. Hence, with above values of t$_2$ and reference distance, the ZFSPs |D| and |E| are obtained for Cr³⁺ at the Cd²⁺ site with distortion having position- Center I: Cd²⁺ (0.4, 0.305, 0.299), Center II: Cd²⁺ (0.6, 0.725, 0.3), Center III: Cd²⁺ (0.7, 0.784, 0.3). The ZFSPs found now are |D| = 0.0758 cm⁻¹, |E| = 0.0033 cm⁻¹ for center I, |D| = 0.0367 cm⁻¹, |E| = 0.0076 cm⁻¹ for center II and |D| = 0.0268 cm⁻¹, |E| = 0.0054 cm⁻¹ for center III, which agree well with the experimental values. The ratio $| b_2^2 | / | b_2^0 |$ = 0.131 and |E| / |D| = 0.043 for center I, $| b_2^2 | / | b_2^0 |$ = 0.621 and |E| / |D| = 0.207 for center II, $| b_2^2 | / | b_2^0 |$ = 0.604 and |E| / |D| = 0.201 for center III, which agree with [26]. Further, with above values of t$_2$ and reference distance, the ZFSPs |D| and |E| are determined for Cr³⁺ at the interstitial site but the values found are very different from the experimental values and so these data are not provided here.

The calculated and experimental ZFSPs for Cr³⁺ ion doped Cs₂CdCl₄ are given in Table 2. It is observed from Table 2 that the ZFSPs |D| and |E| agree well with the experimental ones [9] when the distortion is taken into consideration.

IV.   SPM calculations of CFPs

Employing Wybourne operators [10, 31], the CF energy levels of transition ions doped crystals [27-30] in terms of CF Hamiltonian $\mathcal{H}_{CF}$ [31, 32] are obtained as:

$$\mathcal{H}_{CF} = \sum_{kq} B_{kq} C_q^{(k)} \tag{6}$$

From SPM [15-17], the CFPs, B_{kq} in Eq. (6) for an ML$_n$ complex are given by:

$$B_{kq} = \sum_i \bar{A}_k \left(\frac{R_0}{R_i} \right)^{t_k} K_{kq}\left(\theta_i, \varphi_i\right). \tag{7}$$

where R$_0$ is the reference distance; R$_i$, θ$_i$, φ$_i$ are the spherical polar coordinates of the ith ligand and K$_{kq}$ represent the coordination factors [27]. To obtain B$_{kq}$ (k = 2, 4; q = 0, 2, 4); $\bar{A}_2$ = 40, 400 cm^{-1}, t$_2$ = 1.3, $\bar{A}_4$ =11, 700 cm^{-1} and t$_4$ = 3.4 are taken here [27]. The calculated B$_{kq}$ parameters are shown in Table 3. The ratio B$_{22}$/B$_{20}$ = 0.062 for center I, B$_{22}$/B$_{20}$ = -0.339 for center II and B$_{22}$/B$_{20}$ = -0.492 for center III, show that B$_{kq}$ parameters are standardized [26]. Taking B$_{kq}$ parameters from Table 3 and CFA package [28, 29], the CF energy levels of Cr^{3+} ion in Cs$_2$CdC1$_4$ single crystals are determined. The energy levels of Cr^{3+} ion are calculated by diagonalizing the complete Hamiltonian. The calculated energy values are given in Table 4. As optical absorption data on Cr^{3+}: Cs$_2$CdC1$_4$ could not be found in literature, the experimental energy values for similar ligand crystal Cr^{3+}: MgF$_2$ [33] are taken for comparison here. It is observed from Table 4 that there is reasonable agreement between theoretical and experimental energy values. Therefore the theoretical study of Cr^{3+} ions entering Cs$_2$CdC1$_4$ single crystal at Cd^{2+} sites supports the experimental results [9].

V.   Conclusions

The ZFSPs and the CFPs are evaluated using SPM for Cr^{3+} ions in Cs$_2$CdC1$_4$single crystals. Cr^{3+} ions enter the Cs$_2$CdC1$_4$ single crystal at Cd^{2+} sites with charge compensation. The computed conventional ZFSPs for Cr^{3+} ion at Cd^{2+} sites in Cs$_2$CdC1$_4$ crystal agree well with the experimental values when distortion is taken into consideration. The CF energy values for Cr^{3+} ions at Cd^{2+} sites determined using CFA package and CFPs are in reasonable agreement with the experimental values. Therefore the theoretical results support the experimental observation. Modeling techniques applied here may be useful in future studies to correlate EPR and optical absorption data for other ion-host systems.

Acknowledgement

References

[1].   H. S. Murrieta, J. O. Rubio, G. S. Aguilar, Phys. Rev. B 19(1979)5516.
[2].   D. J. Newman, E. Siegel, J. Phys. C: Solid State Phys. 9(1976)4285.
[3].   A. Leble, J. J. Raousseau, J. C. Fayet, C. Jacoboni, Solid State Commun. 43(1982)773.
[4].   M. G. Brik, N. M. Avram (Eds.), Optical Properties of 3d-Ions in Crystals: Spectroscopy and Crystal Field Analysis, Chapter 3, Springer, Heidelberg, Germany, 2013,   pp. 95-121.
[5].   Z. Y. Yang, C. Rudowicz, Y. Y. Yeung, J. Phys. Chem. Solids 64(2003)887.
[6].   S. Pandey, R. Kripal, A. K.Yadav, M. Açıkgöz, P. Gnutek, C. Rudowicz, J. Lumin. 230(2020)117548.
[7].   S. Siegel, E. Gebert, Acta Cryst. 17(1964)790.
[8].   D. Balz, Naturwissenschaften. 40(1953)241.
[9].   D. Kay, G. L. McPherson, J. Phys. C: Solid State Phys. 14(1981)3247.
[10].   C. Rudowicz, M. Karbowiak, Coord. Chem. Rev. 287(2015)28.
[11].   C. Rudowicz, Magn. Reson. Rev. 13(1987)1; Erratum, C. Rudowicz, Magn. Reson. Rev. 13(1988)335.
[12].   C. Rudowicz, S.K. Misra, Appl. Spectrosc. Rev. 36(2001)11.
[13].   C. Rudowicz, J. Phys. C Solid State Phys. 18(1985)1415; Erratum: C. Rudowicz, J. Phys. C Solid State Phys.18(1985)3837.
[14].   C. Rudowicz, C. Y. Chung, J. Phys. Condens. Matter 16(2004)5825.
[15].   D.J. Newman, B. Ng, Superposition model, Ch. 5 in: D.J. Newman, B. Ng (Eds.), Crystal Field Handbook, Cambridge University Press, UK, , 2000, pp. 83–119.
[16].   D.J. Newman, B. Ng, Rep. Prog. Phys.52(1989)699.
[17].   D.J. Newman, W. Urban, Adv. Phys. 24(1975)793.
[18].   C. Rudowicz, J. Phys. C: Solid State Phys. 20(1987)6033.
[19].   C. Rudowicz, P. Gnutek, M. Açıkgöz, Appl. Spectroscopy Rev. 54(2019)673.
[20].   M. Açıkgöz, Spectrochim. Acta A 86(2012)417
[21].   K.A. Müller, W. Berlinger, J. Albers, Phys. Rev. B 32(1985)5837.
[22].   K.A. Müller, W. Berlinger, J. Phys. C: Solid State Phys. 16(1983)6861.
[23].   M. Heming, G. Lehmann, Chem. Phys. Lett. 80(1981)235.
[24].   T. H. Yeom, Y. M. Chang, C. Rudowicz, Solid State Commun. 87(1993)245.
[25].   E. Siegel, K. A. Muller, Phys. Rev. B 19(1979)109.
[26].   C. Rudowicz, R. Bramley, J. Chem. Phys. 83(1985)5192.

[27]. Y. Y. Yeung, D. J. Newman, Phys. Rev. B 34(1986)2258.
[28]. Y. Y. Yeung, C. Rudowicz, Comp. Chem. 16(1992)207.
[29]. Y. Y. Yeung, C. Rudowicz, J. Comput. Phys. 109(12993)150.
[30]. Y. M. Chang, C. Rudowicz, Y.Y. Yeung, Computers in Physics 8(1994)583.
[31]. B. G. Wybourne, Spectroscopic Properties of Rare Earth, Wiley, New York, USA, 1965.
[32]. B.N. Figgis, A. Hitchman, Ligand Field Theory and its Applications, Wiley-VCH, New York, USA, 2000.
[33]. R. Nistora*a*, L. Andreici, N.M. Avram, Acta Phys. Polon. A, 116(2009)538.

Table and Figure captions:

Table 1. Fractional coordinates of Cr^{3+} ion and spherical co-ordinates (R, θ, ϕ) of ligands in Cs_2CdCl_4 single crystal.

Table 2. Calculated and experimental ZFSPs of Cr^{3+} doped Cs_2CdCl_4 single crystal along with reference distance.

Table 3. B_{kq} parameters of Cr^{3+} doped Cs_2CdCl_4 single crystal.

Table 4. Experimental and calculated energy band positions of Cr^{3+} doped Cs_2CdCl_4 single crystal.

Fig1. The structure of Cs_2CdCl_4 crystal with SAAS.

Table 1

Position of Cr^{3+}	Ligands	Spherical co-ordinates of ligands		
		$R^{Å}$	θ^{0}	ϕ^{0}
ND: Substitutional Cd (0.5, 0.5, 0.5)	Cl I (1)	8.8385	162.6	0
	Cl I (2)	8.8385	162.6	-89.9
	Cl I (3)	2.6294	89.9	-89.9
	Cl I (4)	2.6294	89.9	0
	Cl II (1)	6.9951	147. 8	45.0
	Cl II (2)	11.5690	161.2	45.0
WD: Substitutional Cd (0.5, 0.5, 0.5) Center I	Cl I (1)	5.5617	155.1	-25.9
	Cl I (2)	5.3203	161.4	-71.8
	Cl I (3)	3.7910	26.4	-71.8
	Cl I (4)	4.1232	34.5	-26.0
	Cl II (1)	3.6616	133. 7	37.3
	Cl II (2)	8.0115	160.7	37.3
WD: Substitutional Cd (0.5, 0.5, 0.5) Center II	Cl I (1)	6.0815	146.3	20.5
	Cl I (2)	6.3593	142.7	82.1
	Cl I (3)	5.1209	48.7	82.1
	Cl I (4)	4.7712	44.9	20.5
	Cl II (1)	5.5670	117. 2	50.4
	Cl II (2)	9.0520	146.8	50.4
WD: Substitutional Cd (0.5, 0.5, 0.5) Center III	Cl I (1)	6.4352	141.8	22.0
	Cl I (2)	6.6131	139.9	75.7
	Cl I (3)	5.4328	51.5	75.7
	Cl I (4)	5..2145	49.6	22.0
	Cl II (1)	6.0870	114. 7	48.2
	Cl II (2)	9.3807	143.8	48.2

Center I: Cr^{3+}-Cs^{+}(1), Center II: Cr^{3+}-Li^{+}, Center III: Cr^{3+}-Na^{+},

ND = No distortion, WD = With distortion.

Table 2

	R_0 Å	Calculated ZFS parameters (cm^{-1})			Conventional ZFS parameters (cm^{-1})		
		$\lvert b_2^0 \rvert$	$\lvert b_2^2 \rvert$	$\lvert b_2^2 \rvert / \lvert b_2^0 \rvert$	$\lvert D \rvert$	$\lvert E \rvert$	$\lvert E \rvert / \lvert D \rvert$
ND	2.0	0.0542	1.91E-10	3.53E-09	0.0542	6.38E-07	1.18E-09
					0.1527^e	0.0305^e	0.199
WD Center I	2.0	0.0758	0.0100	0.131	0.0758	0.0033	0.043
					0.0758^e	0.0036^e	0.047
WD Center II	2.0	0.0367	0.0228	0.621	0.0367	0.0076	0.207
					0.0367^e	0.0069^e	0.188
WD Center III	2.0	0.0268	0.0162	0.604	0.0268	0.0054	0.201
					0.0268^e	0.0019^e	0.070

ND = No distortion, WD = With distortion, Center I: Cd^{2+} (0.4, 0.305, 0.299), Center II: Cd^{2+} (0.6, 0.725, 0.3), Center III: Cd^{2+} (0.7, 0.784, 0.3).

^{e} = experimental.

Table 3

	R_0 Å	Calculated B_{kq} (cm^{-1}) Parameters used for CFA package					
		B_{20}	B_{22}	B_{40}	B_{42}	B_{44}	B_{22}/B_{20}
WD Center I	2.0	60145.14	3740.283	-3505.6	703.709	-1128.33	0.062
WD Center II	2.0	12497.97	-4242.37	-3574.31	30.59677	-2358.89	-0.339
WD Center III	2.0	5451.863	-2684.33	-2678.33	-17.5957	-1932.64	-0.492

WD = With distortion.

Table 4

Transition from $^4A_{2g}(F)$	Experimentally observed band (cm^{-1}) [33]]	Calculated energy band from CFA (cm^{-1})		
		Center I	Center II	Center III
$^4T_2g(F)$	14948		12541, 13535, 13928, 14458, 14916, 15108	11970, 12013, 13858, 14619, 14911, 15067
$^2Eg(G)$	15267	16229,16479	15380,15634	15399,15582
$^4T_1g(F)$	20284	19308, 19451, 19689, 22588, 22769, 23771	19004, 19447, 19823, 20590, 21011, 21297	19360, 19783, 19906, 20111, 20213, 20389

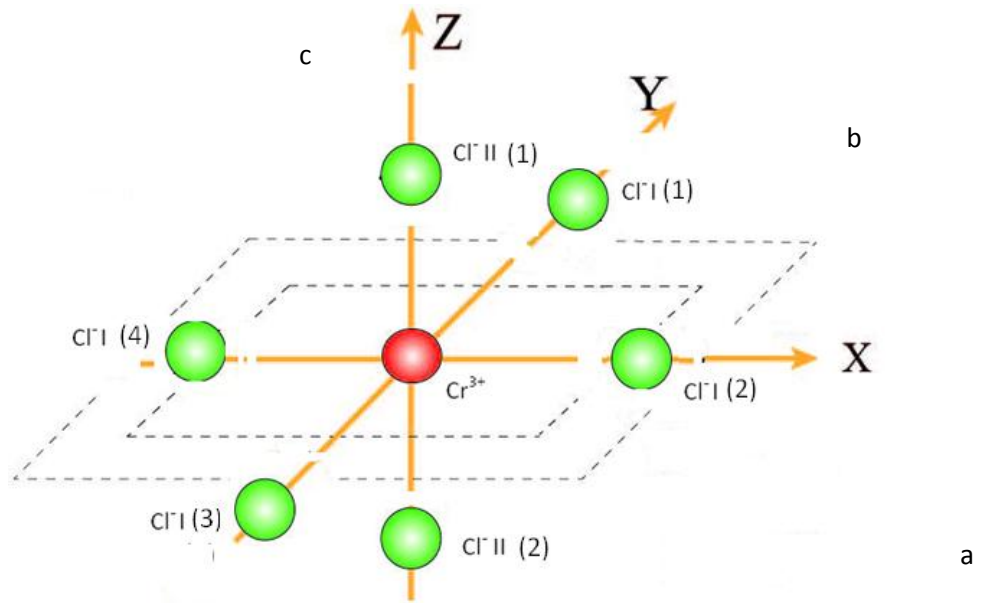(Racah parameters in *A*, *B* and *C*, spin-orbit coupling constant and Trees correction are 0, 516, 3797, 276 and 70 cm^{-1}, respectively)

Fig.1